Chemistry & Biology
Resource

A Near-Infrared BiFC Reporter for In Vivo Imaging of Protein-Protein Interactions

Grigory S. Filonov[1,2] and Vladislav V. Verkhusha[1,*]
[1]Department of Anatomy and Structural Biology and Gruss-Lipper Biophotonics Center, Albert Einstein College of Medicine, Bronx, NY 10461, USA
[2]Present address: Department of Pharmacology, Weill Cornell Medical College, New York, NY 10065, USA
*Correspondence: vladislav.verkhusha@einstein.yu.edu
http://dx.doi.org/10.1016/j.chembiol.2013.06.009

SUMMARY

Studies of protein-protein interactions deep in organs and in whole mammals have been hindered by a lack of genetically encoded fluorescent probes in near-infrared region for which mammalian tissues are the most transparent. We have used a near-infrared fluorescent protein iRFP engineered from a bacterial phytochrome as the template to develop an in vivo split fluorescence complementation probe. The domain architecture-based rational design resulted in an iSplit reporter with the spectra optimal for whole-body imaging, high photostability, and high complementation contrast, which compares favorably to that of other available split fluorescent protein-based probes. Successful visualization of interaction of two known protein partners in a living mouse model suggests iSplit as the probe of choice for noninvasive detection of protein-protein interactions in vivo, whereas its fast intracellular degradation enables time-resolved monitoring of repetitive binding events.

INTRODUCTION

Protein-protein interactions (PPIs) underlie many intracellular processes. Initial investigations of PPIs utilized in vitro techniques such as a coimmunoprecipitation and later advanced to more elaborate approaches capable of PPI detection in live cells. A bimolecular fluorescence complementation (BiFC) is one of the later approaches and is based on the tagging of two proteins with half of a fluorescent protein (FP) each. Upon interaction of these proteins, the two halves of the FP (denoted as split FP) associate with each other to form a fluorescent complex, thus reporting on the PPI. The split protein approach was first proposed and tested for ubiquitin reconstitution (Johnsson and Varshavsky, 1994) and after proving the general concept was applied to a number of enzymes and FPs. The fluorescent split reporters have been engineered using ten different FPs and their mutants (Table 1). Many of them have been applied for studying various PPI events in live cells (Kerppola, 2009); however, certain properties of the current split FPs impose limitations to their use. Split FPs have a tendency for self-association, which decreases the BiFC contrast (Table 1). This has limited the highest reported contrast for cultured cell expression to ~17 for a Venus FP derivative (Kodama and Hu, 2010). Another drawback of many split FPs is a poor maturation at 37°C, limiting their applicability to cells of nonmammalian origin. The latter property worsens in split constructs derived from red FPs, thus hindering multicolor BiFC for the detection of several PPIs simultaneously. Recently, some progress has been made in the engineering of a split mLumin protein (Chu et al., 2009); however, its further validation in mammalian cells is necessary.

Studying PPIs with BiFC in living mammals puts stringent requirements on the properties of the split FP reporter. In addition to good maturation at 37°C, the reporter should possess both excitation and emission maxima inside of a so-called "near-infrared optical window" (NIRW: 650–900 nm) where mammalian tissues are relatively transparent because of low absorption of hemoglobin, melanin, and water in this region. Otherwise, good BiFC contrast observed in vitro will be unacceptably low in vivo due to high tissue autofluorescence caused by endogenous compounds, such as NADPH, flavins, collagen, and elastin. To date, no far-red FPs have been engineered into a BiFC reporter suitable for in vivo imaging. Split mLumin might provide some advance in this direction, although its spectral properties are suboptimal for applications in mammals. Notably, whole-body split reporter-based imaging was successfully facilitated using luciferase (Luker et al., 2004, 2012; Paulmurugan et al., 2002) and thymidine kinase (Massoud et al., 2010), resulting in chemiluminescence and positron emission signals, respectively. However, both types of reporters require injection of exogenous substrates and, in the latter case, provide low contrast and nonspecific signal in vivo.

The high demand for functional in vivo BiFC reporters prompted a search for novel types of protein templates. Recently, two near-infrared fluorescent proteins with both excitation and emission spectra in NIRW engineered from bacterial phytochromes have been reported and expressed in mammals (Filonov et al., 2011; Shu et al., 2009). One of them, iRFP protein (Filonov et al., 2011), appeared to be a good candidate for designing an in vivo PPI probe because it possesses high in vivo brightness and low cytotoxicity and utilizes endogenous concentrations of biliverdin (BV) chromophore to acquire fluorescence. Here, we describe the development, characterization in mammalian cells, and validation of in vivo applicability of a near-infrared split reporter based on iRFP protein.

Table 1. Comparison of Major Properties for Available BiFC Reporters Based on Fluorescent Proteins

Parental FP Used for Engineering BiFC Reporter	Ex/Em Maxima of Parental FP Identity of Ex/Em Maxima with That of BiFC Reporter) (nm)	Interacting Pair Used	BiFC Contrast in Cultured Mammalian Cells (Fold)	Temperature Sensitivity of Maturation of BiFC Reporter	Reference
ECFP	452/478 (yes)	ZIP domains of Fos and Jun	~10 at 30°C	yes (poor maturation at 37°C)	Hu and Kerppola, 2003
EGFP-sg25	475/505 (yes)	Leucine zippers	ND	ND	Ghosh et al., 2000
EGFP	488/507 (no, 490/524)	biotinilated DNA oligonucleotides	ND	ND (experiments were at RT)	Demidov et al., 2006
mKG	494/506 (ND)	leucine zippers, PX with PB1 of $p40^{phox}$	ND	no	Ueyama et al., 2008
		TCF7 with β-catenin, PAC1 with PAC2, PAC3 homodimerization			Hashimoto et al., 2009
Dronpa	503/518 (activated form) (ND)	hHus1 with hRad1	ND	no	Lee et al., 2010
EYFP	514/527 (yes)	ATF2 with Jun, p50 with Fos, p65 with Jun	~10 at 30°C	Yes (poor maturation at 37°C)	Hu et al., 2002
		ZIP domains of Fos and Jun			Hu and Kerppola, 2003
Venus	515/528 (ND)	ZIP domains of Fos and Jun	10 at 37°C	no	Shyu et al., 2006
Venus (V150A)			10 at 37°C		Nakagawa et al., 2011
Venus (I152L)			17 at 37°C		Kodama and Hu, 2010
mRFP1-Q66T	549/570 (ND)	CPC with GL3, BP/KNAT1 with BLH7	15–20 (in plant cells only)	ND (experiments were at 26°C –28°C.)	Jach et al., 2006
mCherry	587/610 (ND)	SV40 large T antigen with p53	ND	yes (poor maturation at 37°C)	Fan et al., 2008
mLumin	587/621 (ND)	ZIP domains of Fos and Jun, EGFR with Grb2, STAT5A with STAT5B	ND	no	Chu et al., 2009
iRFP	690/713 (yes)	E-coil with K-coil, FRB with FKBP	50–80 at 37°C	no	This paper

ND, not determined; RT, room temperature.

RESULTS

iRFP Protein as a Template for the Split Reporter

iRFP has retained two distinct domains PAS and GAF from its parental bacterial phytochrome *Rp*BphP2 (PHY and HisK domains were excluded from the protein on the first stage of the iRFP engineering). This suggested that the products of separating iRFP between the two domains might demonstrate split FP properties. Having aligned the sequence of iRFP with that of *Rp*BphP3 (a close homolog of the iRFP's parental *Rp*BphP2 with a known crystal structure), we proposed that the optimal position for the introduction of polypeptide break would be in an unstructured loop spanning between amino acid residues 120–123 (numbering as in iRFP) between the PAS and GAF domains (Figure S1 available online). To test this in bacteria, independent production of these two domains was facilitated by a plasmid bearing two different promoters (rhamnose and arabinose dependent) (Figure S2A). To induce complex formation of the separated PAS and GAF domains, they were fused to coils (named E-coil and K-coil) previously reported to be capable of interacting with each other with a high affinity (K_d = 63 pM) (De Crescenzo et al., 2003) (Figure S2B). Cotransformation of the dual-promoter plasmid encoding the PAS-E and K-GAF fusion constructs with a plasmid encoding heme oxygenase allowed simultaneous expression of the fusions and production of BV. BV is an exogenous chromophore for iRFP that is necessary for the formation of the fluorescent adduct. Upon induction of transcription of the split fusions, the producing bacterial cells demonstrated a clear fluorescent signal. The fluorescent signal was ~10-fold lower than that of bacteria expressing full-length iRFP yet ~40-fold higher than the signal from the cells producing the PAS and GAF domains not fused to coils (Figure S3A), providing the BiFC contrast of ~40-fold. BiFC contrast is a conventional notion in the field of split reporters that describes the difference between the real, induced signal, and background fluorescence, originated from a nonspecific split reporter complementation. Thus, the separated PAS and GAF domains of the iRFP protein retained their ability to reacquire fluorescent properties upon induced close proximity and had a low nonspecific interaction.

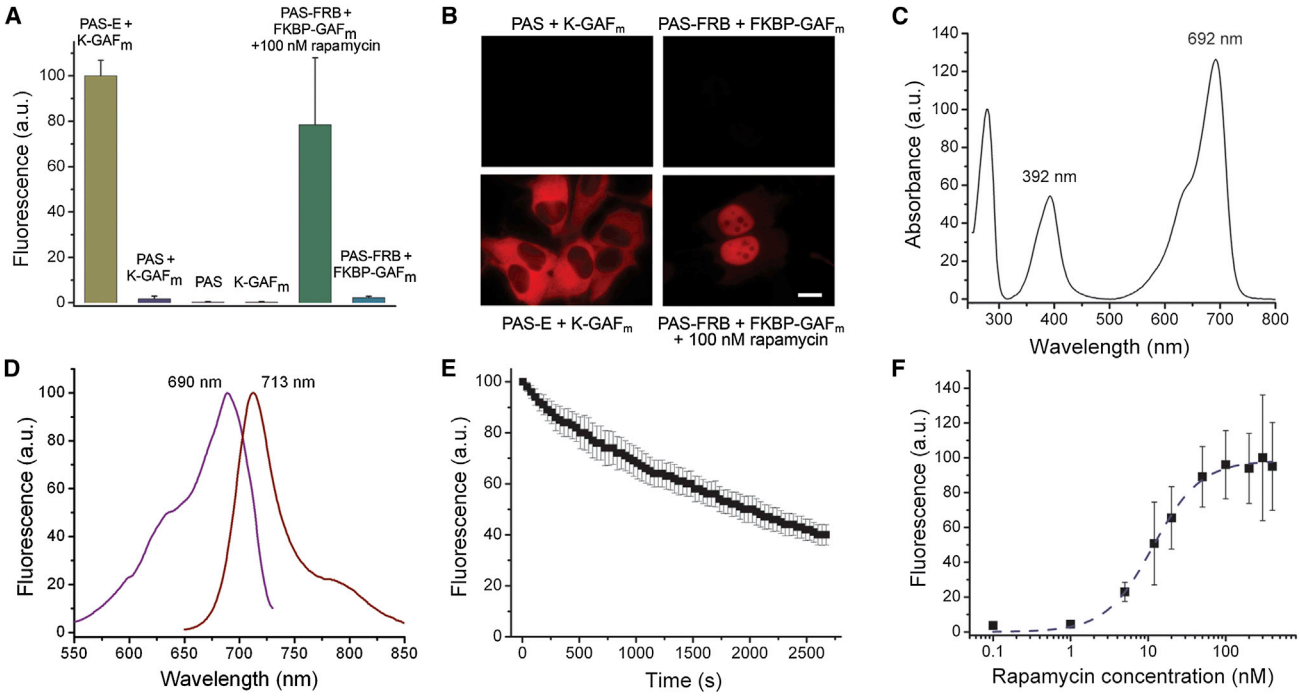

Figure 1. Properties of the iSplit Complex In Vitro and in Cultured Cells

(A) iSplit fluorescence brightness and complementation contrast in cultured cells are shown. HeLa cells were transfected with plasmids encoding the proteins indicated, and the brightness was analyzed using flow cytometry. Rapamycin (100 nM) was added to the culture media 24 hr before the analysis where indicated.

(B) Fluorescence images of the transfected HeLa cells without iSplit formation (top) and after the iSplit complementation (bottom). Scale bar is 20 μm.

(C) Absorbance spectrum of the purified iSplit complex with a peak value at 280 nm set to 100%.

(D) Fluorescence excitation and emission spectra of the purified iSplit complex, normalized to 100%.

(E) Photobleaching of iSplit expressed in HeLa cells measured using Olympus IX81 inverted microscope equipped with a 200 W arc lamp, a 60× 1.35 NA oil immersion objective lens, and a 665/45 nm filter.

(F) Assessing the dissociation constant for the FRB-rapamycin-FKBP complex where FRB or FKBP partners are fused to the iSplit fragments. Different concentration of rapamycin were added to the transfected HeLa cells and incubated for 22 hr followed by FACS analysis. The dashed line is a sigmoidal fitting based on Hill equation ($R^2 = 0.99656$).

See also Figures S1, S2, and S3.

Directed Evolution of the Improved Split Reporter

To increase the brightness of the split iRFP complex in bacteria, we next subjected one of the domains to random mutagenesis. The GAF domain is larger and contains a BV chromophore binding pocket, so we chose to mutate it first. One round of random mutagenesis substantially increased the fluorescent brightness of bacteria producing the split iRFP complexes (Figure S3B). Because the fluorescence brightness of bacteriophytochrome-based FPs in mammalian cells depends on their affinity to endogenous BV (Filonov et al., 2011), we further tested the obtained mutants of the GAF domain in HeLa cells. To accomplish this, the PAS-E and K-GAF (mutant) genes were cloned into two plasmids under the same promoter. Fluorescence-activated cell sorting (FACS) used to compare the mutants in mammalian cells showed that the reconstitution of the split iRFP complexes resulted in bright cell fluorescence at an endogenous BV concentration below ~1 μM (Filonov et al., 2011) (Figure S3C). Although further rounds of random mutagenesis of either the PAS or GAF domains slightly increased brightness of the split complexes, it decreased the iRFP complementation contrast. Thus, we decided to continue with the complex obtained after the first mutagenesis round. This complex, named iSplit, consists of the original PAS domain and GAF domain with three substitutions, which we denoted GAF_m (Figure S1).

Characterization of the Split Reporter in Cells

FACS analysis of the transiently transfected HeLa cells demonstrated that iSplit has a contrast of ~50-fold compared to the control PAS/K-GAF_m pair (Figure 1A). We then chose another protein pair to drive a stimulus-dependent iSplit formation and fused PAS and GAF_m to an N terminus of a FRB protein and a C terminus of a FKBP protein, respectively (Figure S2C). The FRB and FKBP partners interact upon addition of rapamycin (Luker et al., 2004). The induced interaction between the PAS-FRB and FKBP-GAF_m fusion constructs yielded an ~35-fold increase in the HeLa cell brightness. The PAS and GAF_m domains expressed separately or as the PAS/GAF_m combination without induction had a very low fluorescent level close to background (Figure 1A). These results were supported by microscopy imaging of transfected HeLa cells (Figure 1B). An observed nuclear localization of the PAS-FRB/FKBP-GAF_m complex was caused by a nuclear localization signal at the N terminus of the FKBP partner. Exclusion of the PAS-E/K-GAF_m pair from nuclei was possibly caused by the large molecular weight of the iSplit

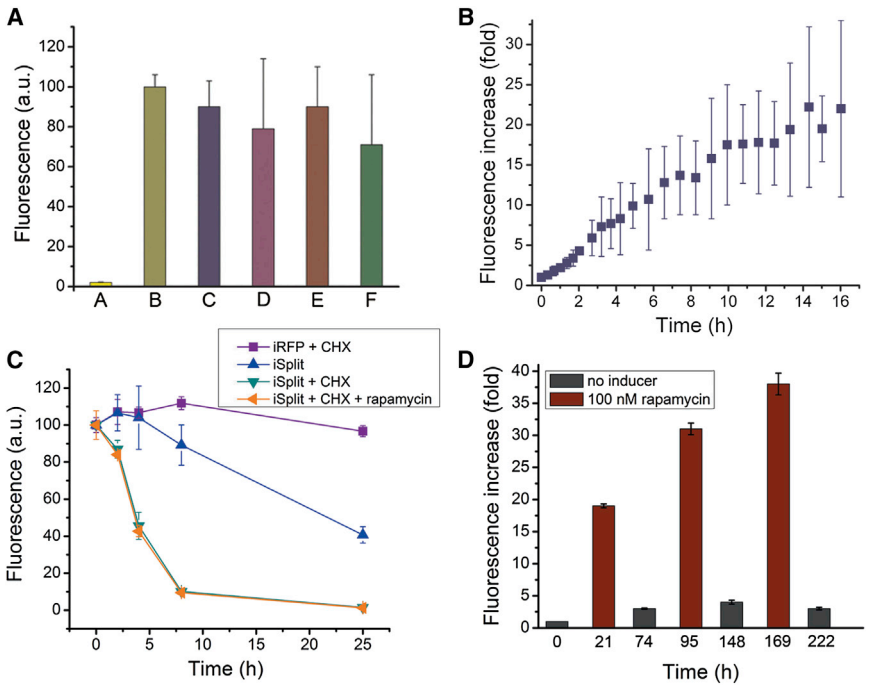

Figure 2. Behavior of the iSplit Complex in Mammalian Cells

(A) Irreversibility of iSplit complex. HeLa cells were transfected with plasmids encoding either the PAS-FRB or FKBP-GAF_m fusion and incubated with 100 nM of rapamycin for 24 hr. Cells in column A were left untreated as a control. Then, these cells (except column B) were washed with PBS, medium was changed, and FK506 (specific competitor of rapamycin) was added to final concentrations of 10 μM (column C), 20 μM (column D), 50 μM (column E), and 100 μM (column F). After incubation for additional 24 hr, all cells were harvested and analyzed with FACS.

(B) Kinetics of the fluorescence increase in MTLn3 preclonal stable cells after addition of 100 nM rapamycin.

(C) Intracellular stability of iSplit in MTLn3 preclonal stable cells in comparison with iRFP. Cells were preincubated with 100 nM rapamycin for 24 hr and then washed (or left with rapamycin) and treated or not with 30 μg/ml cycloheximide (CHX).

(D) Fluorescence brightness of MTLn3 preclonal stable cells expressing iSplit after 100 nM rapamycin addition and washout cycles analyzed by FACS at the indicated time points.

In all panels, error bars represent the 95% confidence intervals calculated based on either three samples in FACS analysis or several cells from three fields of view in microscopy. See also Figures S4 and S5.

complex of ~70 kDa that is beyond the diffusion limit of the nuclear pore (Marfori et al., 2011). Overall, the iSplit complexes did not form aggregates or localize to any specific compartment (Figure 1B).

These results prompted us to study the iSplit spectroscopic properties in more detail. Split iRFP eluted from bacteria has the same absorbance, excitation, and emission peaks as parental iRFP (Figures 1C and 1D). The extinction coefficient, measured by comparison to the absorbance of free BV as previously described (Filonov et al., 2011), provided a value of 85,500 ± 830 $M^{-1}cm^{-1}$, which was slightly lower than an extinction coefficient of 105,000 $M^{-1}cm^{-1}$ for parental iRFP. The quantum yield of iSplit was 6.2% ± 0.5%, which is close to 5.9% of iRFP. The iSplit photostability in live mammalian cells was similar to that of iRFP with the half-time being 33.0 ± 5.2 min (Figure 1E), whereas for iRFP the half-time measured using the same conditions was 26 min (Filonov et al., 2011).

Next, we studied whether the PAS or GAF_m domains separately or combined could affect the binding efficiency of the FRB/FKBP partners. Transfected HeLa cells expressing the PAS-FRB/FKBP-GAF_m complex were incubated with different concentrations of rapamycin and then FACS analyzed to plot a titration curve (Figure 1F). The rapamycin-induced fluorescence intensity of these cells, fitted with a curve based on the Hill equation, showed saturable binding with the EC_{50} being 11.6 ± 0.7 nM, close to the K_d value determined in vitro (12 nM) (Banaszynski et al., 2005). This indicated that the PAS and GAF domains did not affect the binding properties of FRB and FKBP.

In order to evaluate the irreversibility of the iSplit complex formation, HeLa cells expressing the PAS-FRB and FKBP-GAF_m fusions and preincubated with rapamycin were washed and then treated with FK506, which is a competitive inhibitor of the FRB and FKBP interaction. Suitably, even high concentrations of FK506 did not cause a decrease in the fluorescence intensity, thus indicating the irreversible nature of the iSplit formation. BiFC irreversibility is common for other FP-based split partners as well (Shyu and Hu, 2008) (Figure 2A).

Because the main application of iSplit was conceived for in vivo imaging (see below), we made a stable preclonal mixture of the MTLn3 breast adenocarcinoma cells coexpressing E2-Crimson far-red FP (excitation 605 nm, emission 646 nm) (Strack et al., 2009) as a volumetric marker, and the PAS-FRB and FKBP-GAF_m fusions. The stably expressing PAS-FRB/FKBP-GAF_m cells provided a BiFC contrast of up to ~80-fold upon rapamycin addition and brightness of 25% of the MTLn3 cells stably expressing iRFP (Filonov et al., 2012) (Figure S4). We then measured the kinetics of cellular fluorescence upon addition of rapamycin using microscopy (Figure 2B). A BiFC contrast of 10-fold was reached as early as 4.5 hr after addition of rapamycin.

To study the intracellular stability of iSplit, the MTLn3 stable cells preincubated with rapamycin were washed and then either left in the medium only or in the medium with 30 μg/ml cycloheximide. The iSplit complex degraded rapidly with a half-time of ~3.8 hr (Figure 2C). Addition of rapamycin to the cells with cycloheximide resulted in a similar fluorescence decay, indicating that intracellular complex degradation and not complex dissociation caused the fluorescence decrease. Without cycloheximide, the iSplit half-time increased to ~21.6 hr, possibly due to residual rapamycin left in the cells. The control iRFP-expressing cells demonstrated the expected high protein stability (Filonov et al., 2011).

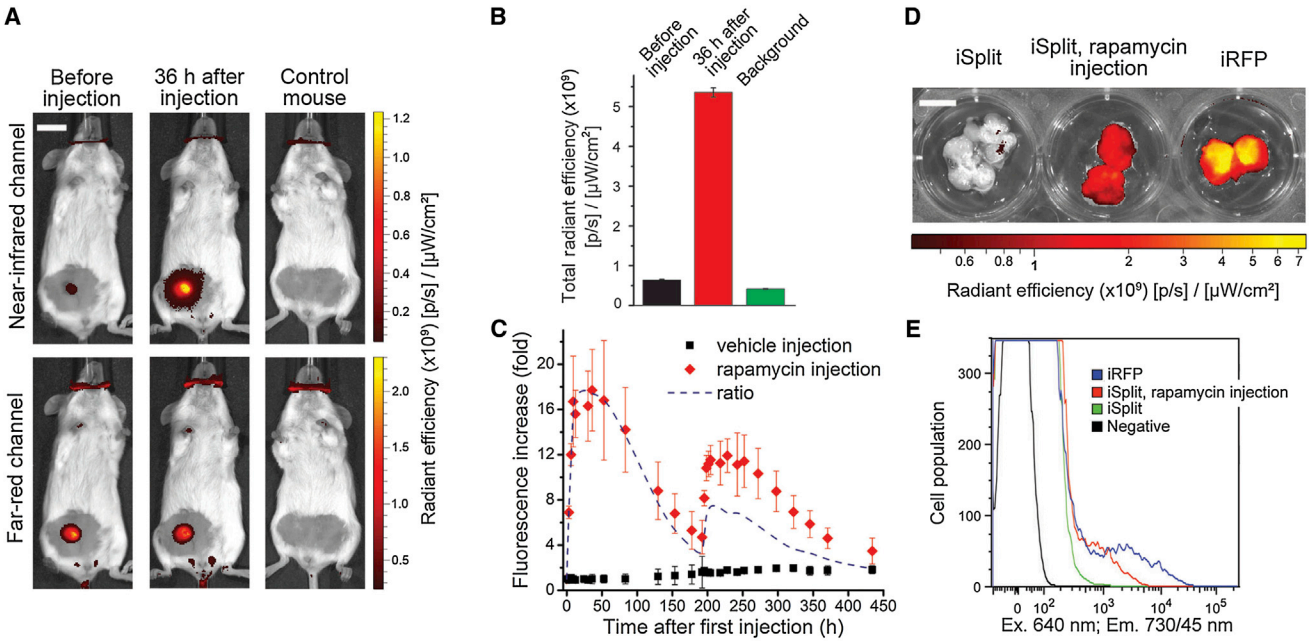

Figure 3. Expression of the iSplit Complex in Living Mice

(A) Representative images of a mouse bearing a 3-week-old MTLn3 tumor coexpressing E2-Crimson and PAS-FRB and FKBP-GAF$_m$ pair before (left image) and 36 hr after (middle image) the rapamycin intraperitonial injection (4.5 mg/kg) imaged in a 675/30–720/20 nm excitation-emission near-infrared channel for iSplit imaging (top) and in a 605/30–660/20 nm excitation-emission far-red channel for tumor volume assessment by means of E2-Crimson fluorescence (bottom). A mouse on the right is the autofluorescence control. Scale bar is 1 cm.

(B) Quantification of the near-infrared fluorescence intensities of the mice in (A). Fluorescence brightness before rapamycin injection (black bar), 36 hr after the injection (red bar), and that of the control mouse (green bar) is shown. Subtraction of the autofluorescence background from the fluorescence signals before and after the rapamycin injection results in ~23-fold difference. Error bars represent the 95% confidence interval calculated based on three subsequent images.

(C) Kinetics of the near-infrared fluorescence change in mice with MTLn3 tumors injected with either rapamycin (red diamonds) or vehicle (black squares). The near-infrared fluorescence intensity for each mouse was normalized to the E2-Crimson far-red signal, and the resulting value was normalized to a value at time 0 hr to plot the fluorescence changes. Error bars represent the SD values of the fluorescent intensity from three mice. Dashed line represents the b-spline fitting of the ratio of fluorescence from the mice injected with rapamycin and with vehicle. The latter normalization takes into the account spontaneously associated iSplit.

(D) Postmortem near-infrared images of the MTLn3 tumors cut in halves shortly after the isolation from mice. The tumors with noncomplemented iSplit (left image), complemented (middle image) iSplit, and expressing iRFP are shown. Scale bar is 1 cm.

(E) FACS analysis of the MTLn3 cells isolated from the tumors in (D).

See also Figures S6 and S7.

These observations suggested that the fast intracellular turnover of the iSplit complex could provide the possibility of studying PPIs several times in the same cells, especially because the timescale of in vivo experiments is typically days. To validate this hypothesis, we used the same MTLn3 cells to turn the iSplit complex formation on and off several times (Figure 2D). The cells were rapamycin pretreated, FACS analyzed, washed out, FACS analyzed after additional time, and rapamycin pretreated again to complete the iSplit complex formation-degradation cycle. Indeed, the fluorescence intensity of the cells showed the anticipated cyclic behavior with some fluorescence increase as the cycles progressed, likely due to intracellular accumulation of rapamycin.

To test whether the iSplit formation is affected by exogenous BV, we added varying BV amounts to either MTLn3 cells coexpressing PAS-FRB/FKBP-GAF$_m$ pretreated with rapamycin or MTLn3 cells expressing iRFP, which possesses a high affinity to BV (Filonov et al., 2011). Both types of cells showed a low fluorescence dependence on the BV level, indicating that iSplit has an affinity to BV similar to that of iRFP and utilizes mostly endogenous BV to exhibit fluorescence (Figure S5).

Performance of the Split Reporter in Live Animals

Having characterized the iSplit properties in vitro and in cultured cells, we utilized MTLn3 cells stably coexpressing E2-Crimson, PAS-FRB, and FKBP-GAF$_m$ to develop a tumor xenograft in living mice (see Experimental Procedures for details). Mice were first imaged 3 weeks after the cancer cell injection. Both the bright signal from E2-Crimson and the faint signal from non-induced iSplit were detected and spectrally resolved without interference (Figures 3A and S6), thus demonstrating the capability of iRFP and its derivatives to be used for two-color in vivo imaging. Upon rapamycin injection, a strong near-infrared fluorescence increase of up to 23-fold at 36 hr after the injection was observed in all animals (Figure 3B), whereas the vehicle injection did not cause fluorescence changes (Figures 3A and 3B).

Figure 3C shows kinetics of the rapamycin-induced fluorescence change normalized to the E2-Crimson fluorescence signal that takes into account differences in the proteins expression level and tumor size. The dashed line represents additional normalization to the spontaneous iSplit association. The iSplit signal reached an average of 18-fold contrast at 40 hr after

rapamycin injection and then decayed during a week (Figure 3C). Another injection of rapamycin into the same mice caused the second wave of the fluorescence increase though with a lower contrast of ~7.5-fold due to the increased nonspecific signal from the accumulated iSplit complex. The decrease of BiFC contrast with time (Figure 3C) does not reflect the fluorescence intensity of the tumors, which, in fact, increased during the course of the experiment (Figure S7).

The postmortem fluorescence intensities of the several-week-old iSplit-expressing tumor, which was rapamycin-induced and excised at maximal brightness, and the iRFP-expressing tumor of similar size differed ~3.2-fold, with iRFP being the higher intensity tumor. Both tumors demonstrated even fluorescence distribution inside (Figure 3D). FACS analysis of cells isolated from these tumors showed decreased fluorescence compared to the original cultured cells (Figures 3E and S4). However, the relative brightness between the iSplit- and iRFP-expressing tumor cells (Figure 2E) remained similar to that obtained in cell culture, suggesting the same low cytotoxicity for iSplit as observed before for iRFP (Filonov et al., 2011).

DISCUSSION

The obtained results have demonstrated that two-domain bacteriophytochrome-derived iRFP is a good candidate for engineering split probes and does not require a laborious search for a position for the polypeptide break as in the case of GFP-like proteins. It is likely that other bacteriophytochrome-based FPs, all having multidomain structures, could be converted into BiFC reporters using similar positions.

iSplit has retained the majority of its parental near-infrared spectral and biochemical properties. With the BiFC contrast of 50- to 80-fold in cultured mammalian cells, iSplit compares favorably to available split reporters based on GFP-like FPs, which may also exhibit poor maturation at 37°C (Table 1), luciferases, and thymidine kinase with maximum intracellular contrasts of 17-fold (Kodama and Hu, 2010), 20- to 75-fold (Villalobos et al., 2010), and ~3-fold (Massoud et al., 2010), respectively. iSplit is the BiFC reporter that has been imaged in a whole animal, moreover, with 18-fold contrast. Compared to luciferase and thymidine kinase, iSplit does not require injection of exogenous substrates. Moreover, fast degradation of iSplit could be beneficial for the visualization of the relatively slow dynamics of PPI in the body, because the fluorescent signal will fade soon after the specific stimulus is gone.

Similar to other PPI systems used in live cells, the iSplit reporter is not precisely quantitative because its fluorescent signal is determined by a number of factors, including PAS and GAF_m domains association, folding and BV-binding kinetics, rates of these proteins' synthesis, and degradation. However, this is the only currently available in vivo PPI reporter system that does not depend on exogenous substrates. Ideally, the iSplit reporter should be used to assess or prove in vivo interaction of proteins, whereas precise measurements of the protein-partners binding properties should be done in vitro with more appropriate techniques.

The difference in the iRFP and iSplit intracellular stabilities can be a result of distinct folding pathways for these proteins. iRFP folds while translated as a single polypeptide chain and this way adopts its intrinsic structure. iSplit is synthesized as two different protein moieties, which likely prefold separately and reach their final conformation once brought into proximity. It is likely that the resulting folds of these proteins have differences, and iSplit possesses some structural elements, which confer its cellular instability. One of these apparent structural differences may be a trefoil knot (Wagner et al., 2005).

To overcome possible negative effects of the irreversibility of the current iSplit variant, a split protein reconstitution based on an intein-mediated protein splicing can be utilized (Paulmurugan et al., 2002). This approach involves incorporation of the intein split fragments into the protein-FP fusion. Once proteins in study interact, the intein halves are brought together and perform protein splicing, which results in ligation of two halves of FP and dissociation of the resulting full-length protein. Because iSplit is an unstable protein, its fluorescent signal should rapidly fade away, whereas the protein partners will now be set free for further biochemical events. This sketch reporter system could be more physiological than the iSplit reporter.

Alternatively, in case of the fast cellular events irreversibly building up, iSplit could allow imaging of transient and low abundant interactions. Also, other more sophisticated complementation strategies suggested for luciferase-based split reporter can also be applied to the iSplit system, thus further expanding its application range (Shekhawat et al., 2009).

Last, the dimeric nature of iRFP, likely inherited by its iSplit derivative, may hinder novel PPI screening but should not be an obstacle in transferring protein complex studies from cell culture to animal models. Other in vivo applications of iSplit could include studies of PPIs in processes at cellular and tissue borders including wound healing, host-pathogen interactions, and organ development. One of the promising applications of iSplit can be its use to extend the GRASP technology and image cell-cell contacts in live mammals (Feinberg et al., 2008).

SIGNIFICANCE

Our work presents the model example of molecular engineering of a bacteriophytochrome based BiFC reporter to study protein-protein interactions. The high contrast of the specific to nonspecific fluorescent signals in the combination with the near-infrared excitation and emission spectra of the iSplit reporter allows detecting interactions in vivo, which has been successfully demonstrated in the mice tumor model.

EXPERIMENTAL PROCEDURES

Plasmid Construction

To generate arabinose and rhamnose inducible plasmids for bacterial expression, the following cloning was done. A pWA21cBP-EGFP-mTagBFP plasmid (see below) was digested with PstI and BglII, and PCR products encoding either a PAS domain of iRFP or the PAS domain fused to an E-coil sequence with the same enzymes were ligated resulting in the pWA-PAS and pWA-PAS-E plasmids, respectively. The plasmids were further digested with NotI and XmaJI. A fragment encoding AraC protein, an arabinose-inducible promoter and a multicloning site linker, was PCR amplified from a pBAD-HisB plasmid (Invitrogen) and digested with the same enzymes. The digested pWA-PAS and pWA-PAS-E plasmids and the PCR fragment were ligated resulting in the pWA-PAS-BAD and pWA-PAS-E-BAD plasmids, respectively. Last, the GAF domain of iRFP and a K-GAF fragment were PCR amplified and

inserted into the latter plasmids via NcoI and KpnI sites to generate pWA-PAS-BAD-GAF and pWA-PAS-E-BAD-K-GAF plasmids, respectively. The E-coil and K-coil sequences were synthesized de novo based on the amino acid sequence (De Crescenzo et al., 2003), and a -ggs- linker was inserted between the coil fragments and the PAS and GAF domains.

A pWA21cBP-EGFP-mTagBFP plasmid was constructed as follows. The gene coding the AraC DNA-binding domain was inserted into the pWA21 plasmid (Wegerer et al., 2008) at BsrGI/HindIII restriction sites after PCR amplification from the pBAD/HisB plasmid (Invitrogen). A pWA21c-AvrIINotI plasmid was next generated by site-specific mutagenesis of the pWA21c plasmid to insert AvrII and NotI sites. The pWA21c-AvrIINotI plasmid was converted into a pWA21cBAD plasmid by cloning the PCR-amplified DNA AvrII/NotI fragment encoding a pBAD promoter into the pWA21C-AvrIINotI plasmid. The pWA21cBAD was then converted into pWA21cBP using site-specific mutagenesis to insert PstI site. Last, the pWA21cBP plasmid was engineered into the pWA21cBP-EGFP-mTagBFP plasmid via inserting of the mTagBFP gene (Subach et al., 2008) at NcoI/KpnI sites. The EGFP gene was present in the original pWA21 plasmid.

A pWA23h plasmid was engineered to provide expression of a heme oxygenase for biliverdin production in bacteria. It contained the rhamnose promoter from the pWA21 plasmid (Wegerer et al., 2008), Kan resistance, and COLA origin parts from a pCOLADuet-1 plasmid (Novagen). First, the AvrII/PciI fragment containing Kan resistance and COLA origin was PCR amplified from pCOLADuet-1 plasmid and inserted into a pWA21h-AvrIINotI vector. Then, a *hmuO* gene encoding *Bradyrhizobium* ORS278 heme oxygenase was PCR amplified from pBAD(hisB)-RpBPhP2-hmuO plasmid (Giraud et al., 2005) and swapped with the EGFP gene in the pWA21-AvrIINotI plasmid.

Mammalian expression of the PAS-E and K-GAF domains for the constitutive complex formation was driven from the plasmids pPAS-E and pK-GAF generated as follows. A pEGFP-C1 plasmid (Clontech) was digested with NheI and BglII and ligated with PCR fragments encoding either the PAS or GAF domains of iRFP fused to the respective coils and digested with the same enzymes. A control pPAS plasmid containing no coil was generated after ligation of the piRFP plasmid (Filonov et al., 2011) digested with NheI and BamHI, and the PCR amplified PAS domain was digested with NheI and BglII.

To generate eight plasmids for the rapamycin dependent interaction of the PAS and GAF containing various fusions, the pC4-RHE or pC4EN-F1 plasmids (ARIAD Pharmaceuticals) encoding FRB or FKBP partners, respectively, were digested with either XbaI or SpeI and ligated with the PCR amplified PAS or GAF domains digested with the same enzymes. The -ggggsggggs- linkers were used between the PAS or GAF domains and the respective partner. The resulting plasmids pC4-RHE-PAS encoding PAS-FRB and pC4EN-F1-GAF_m encoding FKBP-GAF_m were further used.

A pBABE-puro-E2-Crimson plasmid was engineered by inserting E2-Crimson (Strack et al., 2009) DNA digested with EcoRI and SalI into the pBABE-puro plasmid (Morgenstern and Land, 1990) digested with the same enzymes.

Mutagenesis and Screening of Libraries

Random mutagenesis was performed with a GeneMorph II Random Mutagenesis Kit (Stratagene), using conditions that resulted in the mutation frequency of up to 16 mutations per 1,000 base pairs. After the mutagenesis, a mixture of mutants was electroporated into the LMG194 host cells (Invitrogen) containing the pWA23h plasmid. Typical mutant libraries for FACS screening consisted of 10^6–10^8 independent clones. Following the transformation, the LMG194 bacteria were grown for 3 hr in SOC-rich medium and then centrifuged and resuspended in RM medium with 0.002% arabinose, 0.2% rhamnose, 100 μM 5-aminolevulinic acid, and 50 μM $FeCl_3$. The cells were then grown up to 24 hr at 37°C.

For FACS screening, bacteria were washed with phosphate buffered saline (PBS) and then diluted with PBS to an optical density of 0.02 at 600 nm. A MoFlo XDP cell sorter (Beckman Coulter) equipped with standard Ar, Kr, and Ar-Kr mixed-gas lasers was used. Typically, about ten sizes of each library were FACS sorted, using a 676 nm Kr laser line for excitation and a 700LP nm emission filter for positive selection. The brightest collected infrared bacterial cells were rescued in a SOC medium at 37°C for 1 hr and then plated on Petri dishes made of RM/agar supplemented with ampicillin, kanamycin, arabinose, and rhamnose. After overnight expression at 37°C, colonies were analyzed using a Leica MZ16F fluorescence stereomicroscope equipped with the 650/45 nm excitation and 690LP nm emission filters (Chroma). The 20–30 brightest clones were selected, and their DNA was sequenced.

Characterization of Split iRFP Complex In Vitro

The PAS-E/K-GAF complex was produced in the LMG194 bacterial cells as described above and then purified with a Ni-NTA agarose (QIAGEN) using a 6xHis tag attached to the N terminus of the PAS domain. Excitation and emission spectra were measured using a FluoroMax-3 spectrofluorometer (Jobin Yvon). For absorbance measurements, a Hitachi U-2000 spectrophotometer was used. An extinction coefficient was calculated based on a comparison of absorbance values at the main peak at 692 nm with the absorbance value at the 392 nm peak, assuming the latter had extinction coefficient of free BV of 39,900 $M^{-1}cm^{-1}$. To determine a quantum yield, fluorescence signal of the purified iSplit complex was compared to that of an equally absorbing Nile Blue dye.

Cell Culture

HeLa cells were grown in Dulbecco's Modified Eagle Media (DMEM, HyClone) containing 10% fetal bovine serum (FBS), penicillin-streptomycin, and 2 mM glutamine (Life Technologies). Rat adenocarcinoma MTLn3 cells were grown in alpha MEM (Gibco) containing 5% FBS and penicillin-streptomycin. Prior imaging cells were cultured in 35 mm glass-bottom culture dishes with no. 1 cover glasses (MatTek Corporation).

Plasmid transfections were performed using an Effectene reagent (QIAGEN) according to the manufacturer's protocol.

To create stable preclonal mixture of the MTLn3 cells expressing E2-Crimson, the pBABE-puro-E2-Crimson plasmid was used to generate retroviruses, as described (Piatkevich et al., 2010). Upon infection, the MTLn3 cells were maintained with 1.0 μg/ml puromycin (Life Technologies).

Stably expressing cells based on MTLn3 with E2-Crimson were selected with 700 μg/ml G418 following by cotransfection with the pC4-RHE-PAS, pC4EN-F1-GAF_m, and pcDNA3.1 (Invitrogen) (to confer G418 resistance) plasmids. Sorting of positive cells was performed with the MoFlo XDP cell sorter. The collected cells were maintained on both puromycin and G418.

Characterization in Mammalian Cells

To study brightness in mammalian cells, the respective pairs of plasmids were cotransfected. In case of one relevant plasmid needed, the pEGFP-C1 plasmid (Clontech) was used as a mock. In all cases, the pmTagBFP2-C1 plasmid (Subach et al., 2011) was added in a ratio of 1:5 to total plasmid amount to normalize for transfection efficiency. Rapamycin (LC Laboratories) was typically added 24 hr before analysis to the final concentration of 100 nM. Fluorescence intensity of cells was analyzed using a LSRII cytometer (BD Biosciences) equipped with 404, 561, and 640 nm lasers and utilizing 405/50, 610/20, and 730/45 nm filters. To quantify cell fluorescence, a mean fluorescent intensity of the nonnegative population in the near infrared channel was divided by a mean fluorescent intensity of the same population in the blue channel, thus normalizing the near-infrared signal to the transfection efficiency. The analysis also included a compensation of the leakage of the E2-Crimson fluorescence into the near infrared channel. All FACS calculations were performed using FlowJo software (Tree Star).

To assess the FRB/FKBP binding constant, different amounts of rapamycin were added to HeLa cells 40 hr after the transfection and FACS analyzed 22 hr later.

Imaging of HeLa cells was performed 48 hr after the transfection. The HeLa and MTLn3 stably expressing cells were imaged using an Olympus IX81 inverted epifluorescence microscope equipped with LumenPro200 200 W metal-halide arc lamp (Prior), a 60× 1.35 numerical aperture (NA) oil immersion objective lens (UPlanSApo, Olympus), and a standard Cy5.5 filter set (665/45 nm exciter and 725/50 nm emitter) (Chroma). To study fluorescence growth in MTLn3 preclonal mixture coexpressing PAS-FRB/FKBP-GAF_m complex upon 100 nM rapamycin treatment, an environmental chamber with the temperature control (Precision Control) was used to keep the temperature at 37°C.

Photobleaching measurements of the nuclear localized PAS-FRB/FKBP-GAF_m complex (iSplit) in the stable preclonal mixture of MTLn3 cells were

performed after addition of 100 nM rapamycin using the Olympus IX81 microscope, as described (Filonov et al., 2011).

For the protein degradation assay, the stable preclonal mixture of MTLn3 cells expressing PAS-FRB/FKBP-GAF$_m$ complex and incubated with 100 nM rapamycin for 24 hr or stable preclonal mixture of MTLn3 cells expressing iRFP (Filonov et al., 2012) were washed with PBS and then treated with 30 μg/ml of cycloheximide (with addition of 100 nM of rapamycin, where indicated). Cellular brightness was assessed with FACS analysis, as described above.

To study complementation-degradation cycling, the stable preclonal mixture of MTLn3 cells expressing the PAS-FRB/FKBP-GAF$_m$ complex were incubated with 100 nM rapamycin for 21 hr, washed with PBS, split in two parts, and either passed to another dish or FACS analyzed. Nonanalyzed cells were split in two 53 hr after that and either FACS analyzed or treated with 100 nM of rapamycin for an additional 21 hr to start the next cycle.

To check fluorescence dependence on BV concentration, the respective amounts of exogenous BV were added to the stable preclonal mixture of MTLn3 cells expressing PAS-FRB/FKBP-GAF$_m$ complex, preincubated with 100 nM rapamycin for 24 hr, or to the stable preclonal mixture of MTLn3 cells expressing iRFP (Filonov et al., 2012).

In Vivo Fluorescence Imaging

One million MTLn3 cells stably expressing E2-Crimson with the PAS-FRB/FKBP-GAF$_m$ complex, E2-Crimson alone, or iRFP alone were injected into the mammary gland of SCID/NCr mice (female, 5–7 weeks old) (Taconic) and imaged starting 3 weeks later using an IVIS Spectrum instrument (PerkinElmer/Caliper) in epifluorescence mode. Rapamycin was dissolved in 100% ethanol to the concentration of 9 mg/ml and stored at −80°C. Before its intraperitoneal injection, the concentrated stock of rapamycin was diluted in an aqueous solution of 5.2% Tween 80 and 5.2% PEG400. The typical injected volume was 200 μl and resulted in 4.5 mg/kg concentration. The IVIS Spectrum instrument was equipped with 675/30 and 720/20 nm excitation and emission filters for iSplit and iRFP imaging, and 605/30 and 660/20 nm excitation and emission filters for E2-Crimson imaging. Belly fur was removed using a depilatory cream. Mice were fed with AIN-93M Maintenance Purified Diet (TestDiet) to reduce intrinsic autofluorescence level.

The iSplit- and iRFP-expressing MTLn3 tumors were excised postmortem, cut in half, and imaged using the above setup of the IVIS Spectrum instrument. Quantitative measurements of fluorescence signal were made with a Living Image Software 4.0 (PerkinElmer/Caliper). Then, tumors were chopped into pieces, washed with PBS supplemented with 2% of bovine serum albumin, and subsequently filtered through sieves and a 35 μm filter. FACS analysis was performed with the LSRII cytometer using 610/20 and 730/45 nm emission filters.

All animal experiments were performed in an AAALAC approved facility using protocols approved by the Albert Einstein College of Medicine Animal Usage Committee.

SUPPLEMENTAL INFORMATION

Supplemental Information includes seven figures and can be found with this article online at http://dx.doi.org/10.1016/j.chembiol.2013.06.009.

ACKNOWLEDGMENTS

We thank Fedor Subach (currently at the National Research Center Kurchatov Institute, Russia) for the development of the pWA23h plasmid, Erik Giraud (Institute for Research and Development, France) for the *hmuO* gene, Jinghang Zhang for the cell sorting, Yarong Wang for the help with mice, Natalia Zakharova for the help with characterization of the purified reporter, and Kiryl Piatkevich for the useful discussions (all from Albert Einstein College of Medicine). This work was supported by the National Institutes of Health grants GM073913, CA164468, and EB013571.

Received: March 26, 2013
Revised: June 11, 2013
Accepted: June 17, 2013
Published: July 25, 2013

REFERENCES

Banaszynski, L.A., Liu, C.W., and Wandless, T.J. (2005). Characterization of the FKBP.rapamycin.FRB ternary complex. J. Am. Chem. Soc. *127*, 4715–4721.

Chu, J., Zhang, Z., Zheng, Y., Yang, J., Qin, L., Lu, J., Huang, Z.L., Zeng, S., and Luo, Q. (2009). A novel far-red bimolecular fluorescence complementation system that allows for efficient visualization of protein interactions under physiological conditions. Biosens. Bioelectron. *25*, 234–239.

De Crescenzo, G., Litowski, J.R., Hodges, R.S., and O'Connor-McCourt, M.D. (2003). Real-time monitoring of the interactions of two-stranded de novo designed coiled-coils: effect of chain length on the kinetic and thermodynamic constants of binding. Biochemistry *42*, 1754–1763.

Demidov, V.V., Dokholyan, N.V., Witte-Hoffmann, C., Chalasani, P., Yiu, H.W., Ding, F., Yu, Y., Cantor, C.R., and Broude, N.E. (2006). Fast complementation of split fluorescent protein triggered by DNA hybridization. Proc. Natl. Acad. Sci. USA *103*, 2052–2056.

Fan, J.Y., Cui, Z.Q., Wei, H.P., Zhang, Z.P., Zhou, Y.F., Wang, Y.P., and Zhang, X.E. (2008). Split mCherry as a new red bimolecular fluorescence complementation system for visualizing protein-protein interactions in living cells. Biochem. Biophys. Res. Commun. *367*, 47–53.

Feinberg, E.H., Vanhoven, M.K., Bendesky, A., Wang, G., Fetter, R.D., Shen, K., and Bargmann, C.I. (2008). GFP Reconstitution Across Synaptic Partners (GRASP) defines cell contacts and synapses in living nervous systems. Neuron *57*, 353–363.

Filonov, G.S., Piatkevich, K.D., Ting, L.M., Zhang, J., Kim, K., and Verkhusha, V.V. (2011). Bright and stable near-infrared fluorescent protein for in vivo imaging. Nat. Biotechnol. *29*, 757–761.

Filonov, G.S., Krumholz, A., Xia, J., Yao, J., Wang, L.V., and Verkhusha, V.V. (2012). Deep-tissue photoacoustic tomography of a genetically encoded near-infrared fluorescent probe. Angew. Chem. Int. Ed. Engl. *51*, 1448–1451.

Ghosh, I., Hamilton, A.D., and Regan, L. (2000). Antiparallel leucine zipper-directed protein reassembly: application to the green fluorescent protein. J. Am. Chem. Soc. *122*, 5658–5659.

Giraud, E., Zappa, S., Vuillet, L., Adriano, J.M., Hannibal, L., Fardoux, J., Berthomieu, C., Bouyer, P., Pignol, D., and Verméglio, A. (2005). A new type of bacteriophytochrome acts in tandem with a classical bacteriophytochrome to control the antennae synthesis in Rhodopseudomonas palustris. J. Biol. Chem. *280*, 32389–32397.

Hashimoto, J., Watanabe, T., Seki, T., Karasawa, S., Izumikawa, M., Seki, T., Iemura, S., Natsume, T., Nomura, N., Goshima, N., et al. (2009). Novel in vitro protein fragment complementation assay applicable to high-throughput screening in a 1536-well format. J. Biomol. Screen. *14*, 970–979.

Hu, C.D., and Kerppola, T.K. (2003). Simultaneous visualization of multiple protein interactions in living cells using multicolor fluorescence complementation analysis. Nat. Biotechnol. *21*, 539–545.

Hu, C.D., Chinenov, Y., and Kerppola, T.K. (2002). Visualization of interactions among bZIP and Rel family proteins in living cells using bimolecular fluorescence complementation. Mol. Cell *9*, 789–798.

Jach, G., Pesch, M., Richter, K., Frings, S., and Uhrig, J.F. (2006). An improved mRFP1 adds red to bimolecular fluorescence complementation. Nat. Methods *3*, 597–600.

Johnsson, N., and Varshavsky, A. (1994). Split ubiquitin as a sensor of protein interactions in vivo. Proc. Natl. Acad. Sci. USA *91*, 10340–10344.

Kerppola, T.K. (2009). Visualization of molecular interactions using bimolecular fluorescence complementation analysis: characteristics of protein fragment complementation. Chem. Soc. Rev. *38*, 2876–2886.

Kodama, Y., and Hu, C.D. (2010). An improved bimolecular fluorescence complementation assay with a high signal-to-noise ratio. Biotechniques *49*, 793–805.

Lee, Y.R., Park, J.H., Hahm, S.H., Kang, L.W., Chung, J.H., Nam, K.H., Hwang, K.Y., Kwon, I.C., and Han, Y.S. (2010). Development of bimolecular fluorescence complementation using Dronpa for visualization of protein-protein interactions in cells. Mol. Imaging Biol. *12*, 468–478.

Luker, K.E., Smith, M.C., Luker, G.D., Gammon, S.T., Piwnica-Worms, H., and Piwnica-Worms, D. (2004). Kinetics of regulated protein-protein interactions revealed with firefly luciferase complementation imaging in cells and living animals. Proc. Natl. Acad. Sci. USA *101*, 12288–12293.

Luker, K.E., Mihalko, L.A., Schmidt, B.T., Lewin, S.A., Ray, P., Shcherbo, D., Chudakov, D.M., and Luker, G.D. (2012). In vivo imaging of ligand receptor binding with Gaussia luciferase complementation. Nat. Med. *18*, 172–177.

Marfori, M., Mynott, A., Ellis, J.J., Mehdi, A.M., Saunders, N.F., Curmi, P.M., Forwood, J.K., Bodén, M., and Kobe, B. (2011). Molecular basis for specificity of nuclear import and prediction of nuclear localization. Biochim. Biophys. Acta *1813*, 1562–1577.

Massoud, T.F., Paulmurugan, R., and Gambhir, S.S. (2010). A molecularly engineered split reporter for imaging protein-protein interactions with positron emission tomography. Nat. Med. *16*, 921–926.

Morgenstern, J.P., and Land, H. (1990). Advanced mammalian gene transfer: high titre retroviral vectors with multiple drug selection markers and a complementary helper-free packaging cell line. Nucleic Acids Res. *18*, 3587–3596.

Nakagawa, C., Inahata, K., Nishimura, S., and Sugimoto, K. (2011). Improvement of a Venus-based bimolecular fluorescence complementation assay to visualize bFos-bJun interaction in living cells. Biosci. Biotechnol. Biochem. *75*, 1399–1401.

Paulmurugan, R., Umezawa, Y., and Gambhir, S.S. (2002). Noninvasive imaging of protein-protein interactions in living subjects by using reporter protein complementation and reconstitution strategies. Proc. Natl. Acad. Sci. USA *99*, 15608–15613.

Piatkevich, K.D., Hulit, J., Subach, O.M., Wu, B., Abdulla, A., Segall, J.E., and Verkhusha, V.V. (2010). Monomeric red fluorescent proteins with a large Stokes shift. Proc. Natl. Acad. Sci. USA *107*, 5369–5374.

Shekhawat, S.S., Porter, J.R., Sriprasad, A., and Ghosh, I. (2009). An autoinhibited coiled-coil design strategy for split-protein protease sensors. J. Am. Chem. Soc. *131*, 15284–15290.

Shu, X., Royant, A., Lin, M.Z., Aguilera, T.A., Lev-Ram, V., Steinbach, P.A., and Tsien, R.Y. (2009). Mammalian expression of infrared fluorescent proteins engineered from a bacterial phytochrome. Science *324*, 804–807.

Shyu, Y.J., and Hu, C.D. (2008). Fluorescence complementation: an emerging tool for biological research. Trends Biotechnol. *26*, 622–630.

Shyu, Y.J., Liu, H., Deng, X., and Hu, C.D. (2006). Identification of new fluorescent protein fragments for bimolecular fluorescence complementation analysis under physiological conditions. Biotechniques *40*, 61–66.

Strack, R.L., Hein, B., Bhattacharyya, D., Hell, S.W., Keenan, R.J., and Glick, B.S. (2009). A rapidly maturing far-red derivative of DsRed-Express2 for whole-cell labeling. Biochemistry *48*, 8279–8281.

Subach, O.M., Gundorov, I.S., Yoshimura, M., Subach, F.V., Zhang, J., Grüenwald, D., Souslova, E.A., Chudakov, D.M., and Verkhusha, V.V. (2008). Conversion of red fluorescent protein into a bright blue probe. Chem. Biol. *15*, 1116–1124.

Subach, O.M., Cranfill, P.J., Davidson, M.W., and Verkhusha, V.V. (2011). An enhanced monomeric blue fluorescent protein with the high chemical stability of the chromophore. PLoS ONE *6*, e28674.

Ueyama, T., Kusakabe, T., Karasawa, S., Kawasaki, T., Shimizu, A., Son, J., Leto, T.L., Miyawaki, A., and Saito, N. (2008). Sequential binding of cytosolic Phox complex to phagosomes through regulated adaptor proteins: evaluation using the novel monomeric Kusabira-Green System and live imaging of phagocytosis. J. Immunol. *181*, 629–640.

Villalobos, V., Naik, S., Bruinsma, M., Dothager, R.S., Pan, M.H., Samrakandi, M., Moss, B., Elhammali, A., and Piwnica-Worms, D. (2010). Dual-color click beetle luciferase heteroprotein fragment complementation assays. Chem. Biol. *17*, 1018–1029.

Wagner, J.R., Brunzelle, J.S., Forest, K.T., and Vierstra, R.D. (2005). A light-sensing knot revealed by the structure of the chromophore-binding domain of phytochrome. Nature *438*, 325–331.

Wegerer, A., Sun, T., and Altenbuchner, J. (2008). Optimization of an E. coli L-rhamnose-inducible expression vector: test of various genetic module combinations. BMC Biotechnol. *8*, 2.

Chemistry & Biology, Volume *20*

Supplemental Information

A Near-Infrared BiFC Reporter for In Vivo Imaging of Protein-Protein Interactions

Grigory S. Filonov and Vladislav V. Verkhusha

Inventory of Supplemental Information

SUPPLEMENTAL DATA

SUPPLEMENTAL REFERENCES

SUPPLEMENTAL DATA

Figure S1, related to Figure 1.

Alignment of the amino acid sequences of iSplit with parental iRFP.

```
          1         10         20         30         40         50         60
iRFP      MAEGSVARQPDLLTCDDEPIHIPGAIQPHGLLLALAADMTIVAGSDNLPELTGLAIGALIG
PAS       MAEGSVARQPDLLTCDDEPIHIPGAIQPHGLLLALAADMTIVAGSDNLPELTGLAIGALIG
GAFm      ............................................................

                 70         80         90        100        110        120
iRFP      RSAADVFDSETHNRLTIALAEPGAAVGAPITVGFTMRKDAGFIGSWHRHDQLIFLELEPP
PAS       RSAADVFDSETHNRLTIALAEPGAAVGAPITVGFTMRKDAGFIGSWHRHDQLIFLELEPP
GAFm      ............................................................PP

                 130        140        150        160        170        180
iRFP      QRDVAEPQAFFRRTNSAIRRLQAAETLESACAAAAQEVRKITGFDRVMIYRFASDFSGEV
PAS       ............................................................
GAFm      QRDVAEPQAFFRRTNSAIRRLQAAETLESACAAAAQEVRKITGYDRVMIYRFASDFSGEV

                 190        200        210        220        230        240
iRFP      IAEDRCAEVESKLGLHYPASTVPAQARRLYTINPVRIIPDINYRPVPVTPDLNPVTGRPI
PAS       ............................................................
GAFm      IAEDRCAEVESKLGLHYPASTVPAQARRLYTINPVRIIPDINYRPVPVTPYLNPVTGRPI

                 250        260        270        280        290        300
iRFP      DLSFAILRSVSPVHLEFMRNIGMHGTMSISILRGERLWGLIVCHHRTPYYVDLDGRQACE
PAS       ............................................................
GAFm      DLSFAILRSVSPVHLEFMRNIGMHGTMSISILRGERLWGLIVCHHRTPYYVDLDGRQACE

                  310
iRFP      LVAQVLAWQIGVMEE
PAS       ...............
GAFm      LVAQVLARQIGVMEE
```

An original iRFP protein was cut in a loop between the PAS (blue font) and GAF (red font) domains determined according to a crystal structure of the close homologue *Rp*BphP3 (Yang, et al., 2007). The amino acid changes introduced into the GAF domain (resulting in GAF_m) after random mutagenesis are highlighted in yellow.

Figure S2, related to Figure 1.

Schemes of the plasmid for iSplit mutagenesis and its protein fusions.

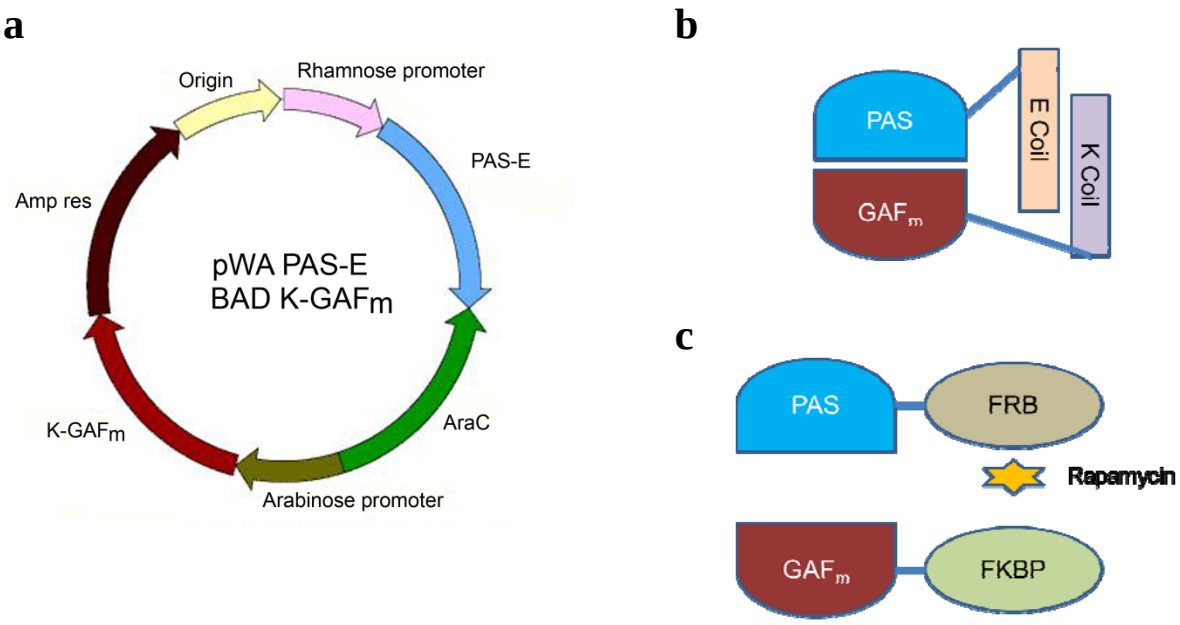

To express the PAS and GAF domains in bacterial cells both genes were cloned onto a single plasmid (**a**) under either arabinose- or rhamnose-induced promoters and introduced into *E. coli* along with another plasmid (see Experimental Procedures) encoding heme oxygenase to produce a BV chromophore. In the course of this study PAS and GAF domains were fused either to the E- or K-coils (De Crescenzo, et al., 2003) to promote constitutive binding following translation (**b**) or to the FRB or FKBP proteins (Banaszynski, et al., 2005) allowing inducible interaction upon addition of rapamycin (**c**).

Figure S3, related to Figure 1.

Initial assessment of split iRFP properties in bacteria and comparison the GAF domain mutants in bacteria and mammalian cells.

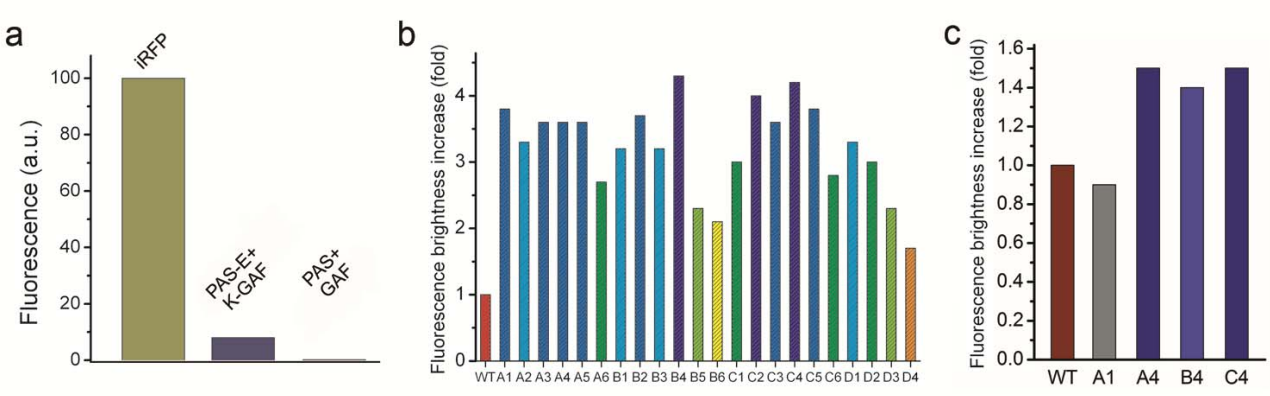

(**a**) Initial expression of the PAS and GAF domains (both with the sequences identical to the ones of iRFP) in bacteria showed that when brought into proximity these domains produce fluorescent complex with a brightness being one tenth of that of parental iRFP. (**b**) Random mutagenesis of the GAF domain generated a series of the mutants with the fluorescence brightness in bacteria being substantially higher than for the initial PAS / GAF pair (indicated as WT). (**c**) The PAS domain and mutants of the GAF domain, which provided the brightest signal in bacteria, were re-cloned into mammalian plasmids and their performance was assessed in HeLa cells to choose the optimal pair: PAS (identical to one in iRFP) + GAF_m (mutant C4). Fluorescence in bacteria was measured in bacterial suspension and normalized to optical density. Fluorescence in mammalian cells was studied using FACS as described in the Experimental Procedures.

Figure S4, related to Figure 2.

FACS analysis of the rapamycin induced iSplit formation in the stable preclonal mixtures of MTLn3 cells.

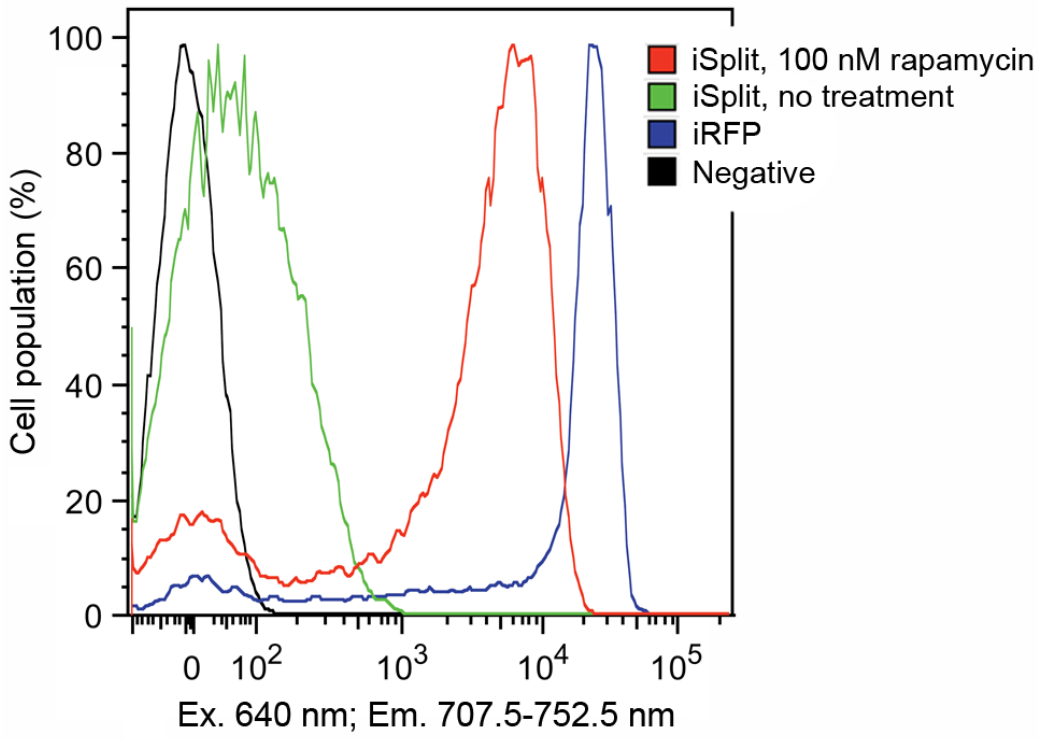

The stable preclonal mixture of MTLn3 cells co-expressing E2-Crimson, PAS-FRB, and FKBP-GAF_m fusions were generated as described in the Experimental Procedures. Cells were pre-incubated with 100 nM of rapamycin for 24 h and then compared to the untreated cells using FACS. The non-expressing cells were used as a negative control, and the stable preclonal mixture of MTLn3 cells expressing iRFP (Filonov, et al., 2012) was used as a positive control.

Figure S5, related to Figure 2.

Assessment of BV binding to the iSplit complex.

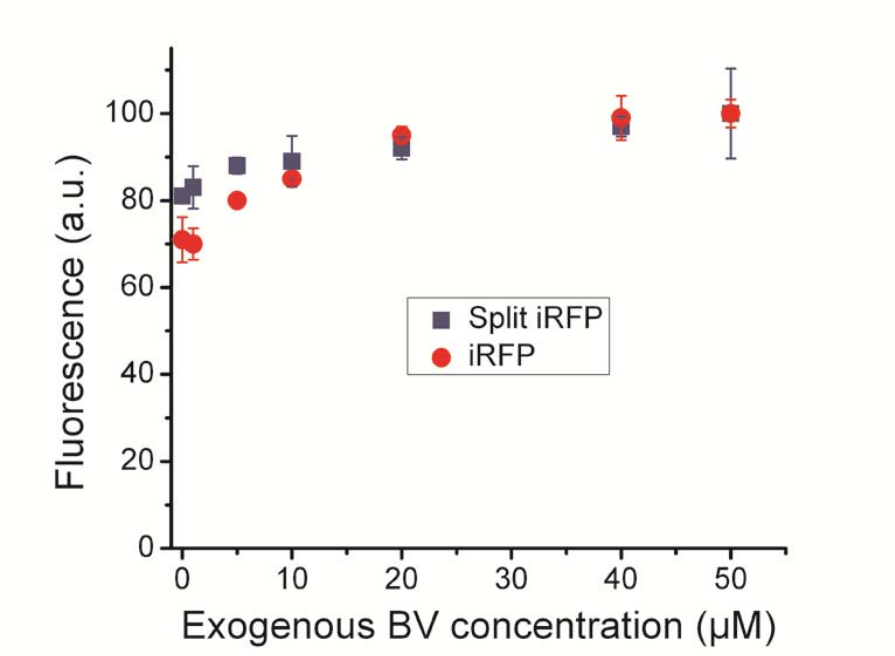

Effect of addition of exogenous BV on cellular fluorescence of MTLn3 preclonal mix expressing either iSplit (pre-treated with 100 nM rapamycin for 24 h) or iRFP was studied. Cells were incubated with the respective amounts of BV for 2 h before FACS analysis. Both iRFP and iSplit complex exhibited a low fluorescence dependence on the increasing amount of exogenous BV and efficiently utilized endogenous BV to achieve their steady fluorescence level. Error bars represent 95% confidence interval calculated based on either 3 samples.

Figure S6, related to Figure 3.

Initial assessment of the iSplit performance *in vivo*.

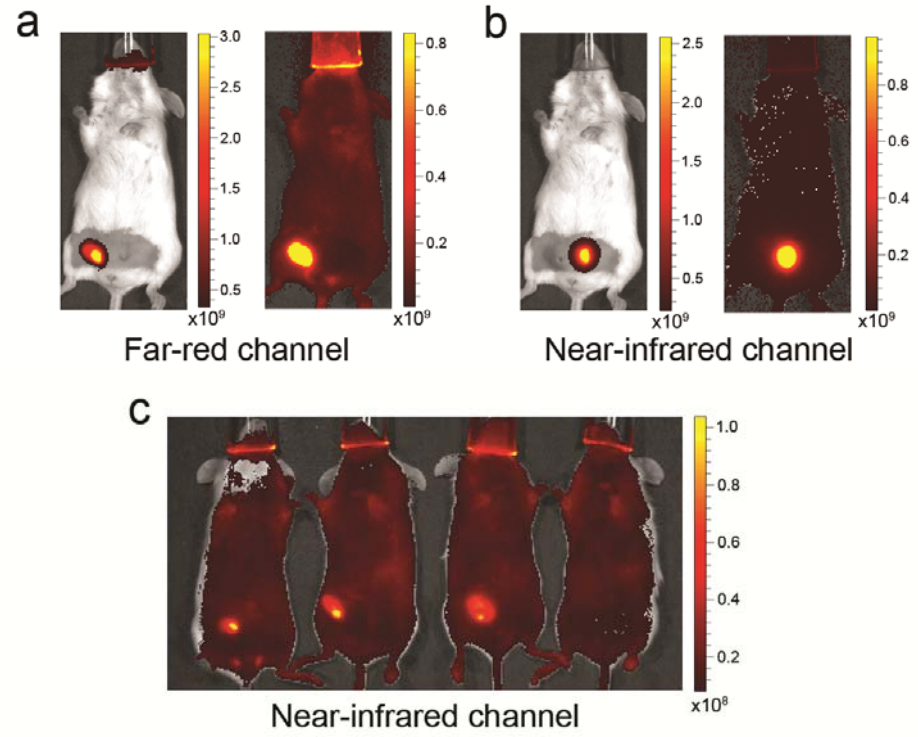

To ensure that there is no spectral crosstalk between E2-Crimson and iSplit signals we imaged a control mouse bearing two tumors. MTLn3 cells stably expressing E2-Crimson only were injected into a mammary gland on the right part of the body and iRFP only stably expressing MTLn3 cells (Filonov, et al., 2012) were injected into a mammary gland on the left part of the body. Imaging started 4 weeks later using the IVIS Spectrum equipped with the 605/30 nm and 660/20 nm (for E2-Crimson) and 675/30 nm and 720/20 nm (for iRFP) filter sets (**a** and **b,** respectively). One can see that both signals are spectrally resolved with no detectable crosstalk even when the display range of fluorescence intensity is broaden to visualize autofluorescence (right image in each panel). This experiment allowed to attribute the signal observed in E2-Crimson / PAS-FRB / FKBP-GAF_m co-expressing tumor in mice before rapamycin injection to the real background signal from the spontaneously associated PAS-FRB / FKBP-GAF_m pair and, thus, to quantify the signals appropriately (panel **c**, mouse on the right is a control one without a tumor).

Figure S7, related to Figure 3.

Increase of raw fluorescent intensity in the rapamycin injected mouse.

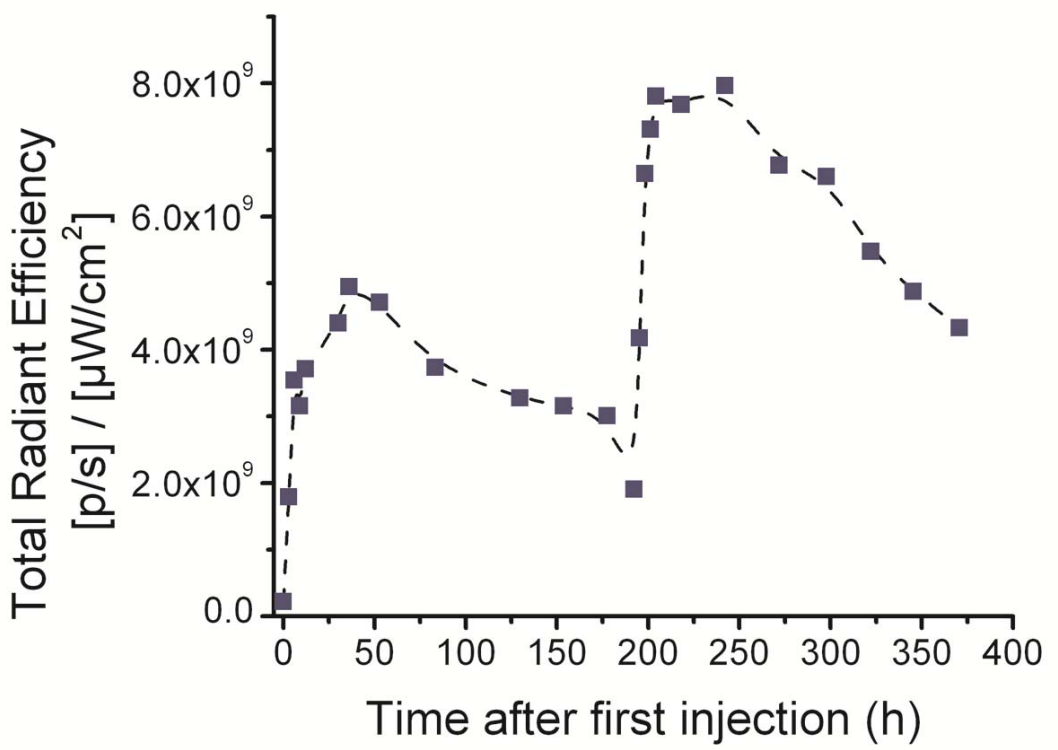

A representative mouse from Figure 3a was imaged using the IVIS Spectrum instrument as described in Methods, and raw fluorescent data from the near-infrared channel was plotted as a function of time after the first injection of rapamycin. The second rapamycin injection was made at the time point of 192 hours after the first one. Overall signal shows a steady increase due to the growth of the tumor volume and possible accumulation of non-specifically complemented iSplit complex.

SUPPLEMENTAL REFERENCES

Banaszynski, L.A., Liu, C.W., and Wandless, T.J. (2005). Characterization of the FKBP.rapamycin.FRB ternary complex. Journal of the American Chemical Society 127, 4715-4721.

De Crescenzo, G., Litowski, J.R., Hodges, R.S., and O'Connor-McCourt, M.D. (2003). Real-time monitoring of the interactions of two-stranded de novo designed coiled-coils: effect of chain length on the kinetic and thermodynamic constants of binding. Biochemistry 42, 1754-1763.

Filonov, G.S., Krumholz, A., Xia, J., Yao, J., Wang, L.V., and Verkhusha, V.V. (2012). Deep-tissue photoacoustic tomography of a genetically encoded near-infrared fluorescent probe. Angew Chem Int Ed Engl 51, 1448-1451.

Yang, X., Stojkovic, E.A., Kuk, J., and Moffat, K. (2007). Crystal structure of the chromophore binding domain of an unusual bacteriophytochrome, RpBphP3, reveals residues that modulate photoconversion. Proc Natl Acad Sci U S A 104, 12571-12576.